LBNL-39457
UC-414

CONF-9608172--1

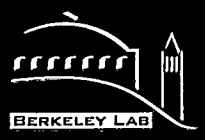

ERNEST ORLANDO LAWRENCE
BERKELEY NATIONAL LABORATORY

Recent Results from Hadronic Observables at the CERN SPS

P.M. Jacobs for the NA49 Collaboration
Nuclear Science Division

October 1996
Presented at *HIPAGS '96*,
(Heavy Ion Physics at the AGS),
Detroit, MI,
August 22–24, 1996,
and to be published in
the Proceedings

LBNL-39457
UC-414

Recent Results from Hadronic Observables at the CERN SPS

Peter M. Jacobs

Nuclear Science Division
Ernest Orlando Lawrence Berkeley National Laboratory
University of California
Berkeley, California 94720

for the NA49 Collaboration

Athens, Berkeley Lab, Birmingham, RMKI Budapest, CERN, GSI, UC Davis,
JINR Dubna, IKF Frankfurt, IFJ Krakow, UCLA, Marburg, MPI Munich,
U. of Washington, IPJ Warsaw, U. Warsaw, IRB Zagreb

October 1996

This work was supported by the U.S. Department of Energy under Contract No. DE-AC03-76SF00098.

DISCLAIMER

Recent Results from Hadronic Observables at the CERN SPS

Peter M. Jacobs
Lawrence Berkeley National Laboratory,
MS 50A-1148, 1 Cyclotron Road,
Berkeley CA 94720

for the NA49 Collaboration:

Athens–LBNL–Birmingham–RMKI Budapest–CERN–GSI–UC Davis– JINR Dubna–IKF Frankfurt–IFJ Krakow–UCLA–Marburg–MPI Munich– U. of Washington–IPJ Warsaw–U. Warsaw–IRB Zagreb

ABSTRACT

Some recent results on Pb+Pb collisions from NA44 and NA49 at the CERN SPS are reviewed and compared to collisions of lighter systems and lower energies. For central collisions: primordial protons show enhanced stopping for Pb+Pb relative to S+S at the same energy, but less stopping than heavy systems at lower energy; yields of negative hadrons, kaons and lambdas scale with the number of participants relative to S+S; and transverse momentum spectra show strong evidence for enhanced radial flow in the heaviest system. For intermediate impact parameters, significant quadrupole deformation of the transverse energy distribution is seen at mid–rapidity. Coulomb effects are seen for central collisions in the ratio of yields π^-/π^+ and unlike–sign two particle correlations.

1. Introduction

Beams of lead ions at 158 GeV/nucleon became available at the CERN SPS in November 1994, representing the culmination of the CERN fixed target heavy ion program, which had run since 1986 with beams of oxygen and sulphur ions. The principal goal of this program is the investigation of states of highly excited matter, with the hope of observing the phase transition from hadronic to quark-gluon matter. Qualitative arguments indicate that collisions of the heaviest systems are most favourable for this study:

- Increasing the radius of the colliding ions by almost a factor two (lead relative to sulphur) leads to a larger reaction volume and consequently longer lifetime of the hot system, with greater opportunity to achieve equilibrium at the center of the collision region.

- Projection of a lead nucleus onto a two–dimensional plane gives a mean transverse spacing of nucleons of about 0.6 fm., which will consequently be the mean transverse spacing of adjacent strings extending from the receding participants. New collective inter–string effects may therefore occur.

It of course remains for the experiments to determine whether new and interesting effects are seen. Many analyses of data from lead beams are now reaching maturity. The most exciting recent news is the possible observation of a threshold behaviour in the suppression of the J/ψ in Pb+Pb collisions. This result remains controversial, however, and I will not report on it here. See instead the primary [1], secondary [2], tertiary [3], and quaternary [4] sources.

I will concentrate instead on some aspects of the collision seen through the final state hadrons. These include: stopping as measured by the primordial proton distribution; meson and baryon yields and p_T distributions, which address questions such as entropy production, strangeness production, and radial flow; azimuthal asymmetry of the final state seen through the transverse energy distribution; and unlike–sign two particle correlations, which are sensitive to Coulomb effects and the spatial extent of the source. Due to lack of space I will not discuss the rapidly evolving field of identical two-particle correlations, whose parameters seem to grow with those of the ions being studied [5].

All Pb+Pb data presented here from NA44 and NA49 are preliminary.

2. Single Particle Spectra

Stopping in Central Collisions: The final state rapidity distribution of primordial protons is a measure of the *stopping* of initial baryons [6] and therefore indicative of the net baryon density and energy available to excite matter at midrapidity. By primordial we mean those protons not produced in the collision (which are equal in number to the observed antiprotons) or those resulting from the decay of heavier baryons (whose decay kinematics will distort the $y - p_T$ distribution).

Fig. 1 shows the rapidity density of primordial protons measured by NA49 as a function of rapidity for central collisions ($\sigma_{cent} = .05\sigma_{inel}$). The distribution is the difference in yields between all positive and negative hadrons ("plus minus minus"), with rapidity calculated assuming the proton mass. Corrections are made for the difference in yield between positive and negative pions and kaons, as well as decays from Λ and $\overline{\Lambda}$. Also shown is the same distribution for central S+S collisions measured by NA35 [7] scaled in magnitude by a factor 6.6, which is the ratio of numbers of participants (with a small correction for the differing beam energies). Comparison of the shapes of the distributions shows that the lead collisions have somewhat greater stopping, in agreement with the measurement of transverse energy at midrapidity [8].

Fig. 2 shows the same Pb+Pb data as Fig. 1, but compared to equivalent distributions from collisions of heavy systems at the Bevalac (1.15 GeV/nucleon) [9] and AGS (10.6 GeV/nucleon) [10], scaled by the beam rapidity for comparison. At the Bevalac, the primordial proton distribution is strongly peaked at midrapidity, indicating full stopping. Scaling of the distribution with increasing beam rapidity is not observed. Rather, a flattening of

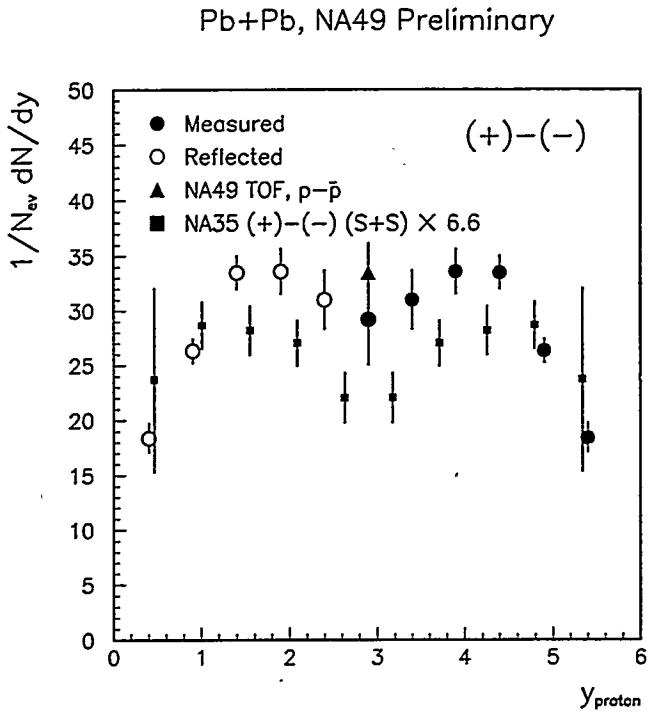

Figure 1: Mass dependence of proton stopping. Filled circles are the NA49 "plus minus minus" dN/dy (TPC data); open circles are the same data reflected about mid–rapidity; triangle is an independent NA49 TOF measurement of identified protons and antiprotons, not corrected for Λ daughters; filled squares are the NA35 "plus minus minus" measurement for S+S. Error bars include an estimate of systematic errors.

the distribution, i.e. an increase in transparency or longitudinal flow, is seen with increasing energy.

Hadron Rapidity Distributions in Central Collisions: Fig. 3 shows the rapidity density of negative hadrons ($\pi^-, K^-, \overline{p}$) for central Pb+Pb collisions measured by NA49, as a function of rapidity. Superimposed is the equivalent distribution for S+S collisions [7] scaled by the factor 6.6 corresponding to the ratio of numbers of participants for central collisions. The level of agreement using this scaling is striking. Yields of K^+, K^-, and K^0_s as measured by NA49 and NA35 [11] also exhibit scaling with number of participants, though the spectra have estimated systematic errors of 30%. The simplest interpretation of this scaling is that secondary particle production is dominated by hadronic, as opposed to collective nuclear, mechanisms [12].

Inverse Slope Parameters at Mid–Rapidity in Central Collisions: Table 1 summarizes inverse slope parameters measured by NA44 and NA49 at mid–rapidity for central S+S and Pb+Pb collisions. The level of (dis)agreement between the experiments gives an idea of the systematic errors, and may in part be due to different fitting procedures. However, the clear message from Table 1 is that the inverse slope parameters for the heaviest particles increase considerably for the heavy system, symptomatic of increased radial flow.

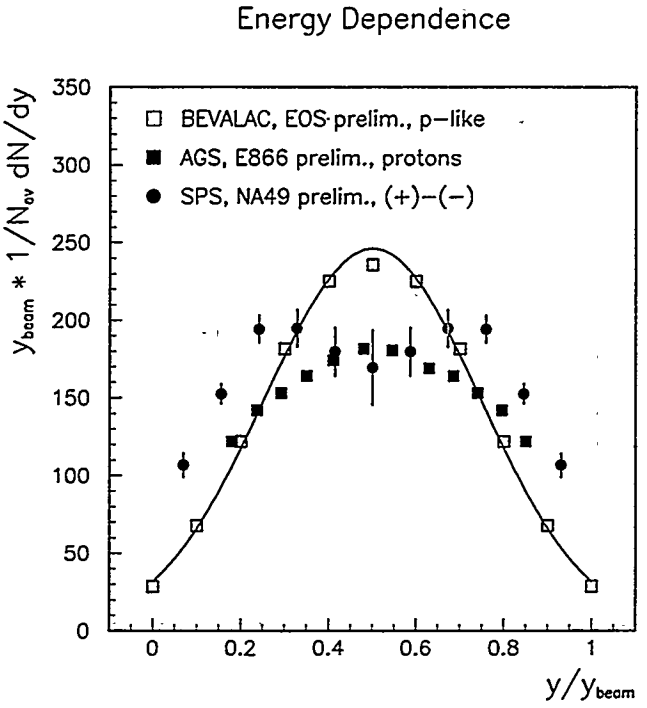

Figure 2: Energy dependence of proton stopping: rapidity density dN/dy scaled by beam rapidity. Open squares are EOS (Bevalac) p–like ("p–like" accounts for the fraction of baryons carried by fragments); curve is a Gaussian fit to these data to illustrate their Gaussian nature; filled squares are identified protons from E866 (AGS); filled circles are the NA49 TPC data from Fig. 1.

Together with Fig. 1, a picture emerges from the data for the heavy system of increased stopping leading to greater energy available at mid–rapidity, some of which is taken up by greater collective radial expansion. This picture may be quantified by a systematic study of all available data within the framework of one of the various hydrodynamic codes now on the market [13].

3. Azimuthal Correlation of Transverse Energy

Directed flow of transverse energy (finite dipole moment of the azimuthal E_T distribution) has been observed at the AGS [15]. NA49 has observed a finite quadrupole moment of the azimuthal E_T distribution near mid–rapidity at the SPS [16]. Data were taken by NA49 using the Ring Calorimeter in a special run without magnetic field, with the calorimeter spanning the pseudorapidity range $2.1 < \eta < 3.8$. The calorimeter is subdivided into 10 radial rings and 24 azimuthal wedges, making 240 cells in total. To study azimuthal correlations, disconnected rings were chosen forward and backward of mid-pseudorapidity, spanning $2.1 < \eta < 2.6$ and $3.3 < \eta < 3.8$. It is essential that the rings be separated to prevent cross–talk between calorimeter cells. In each event, a transverse energy tensor is defined for each

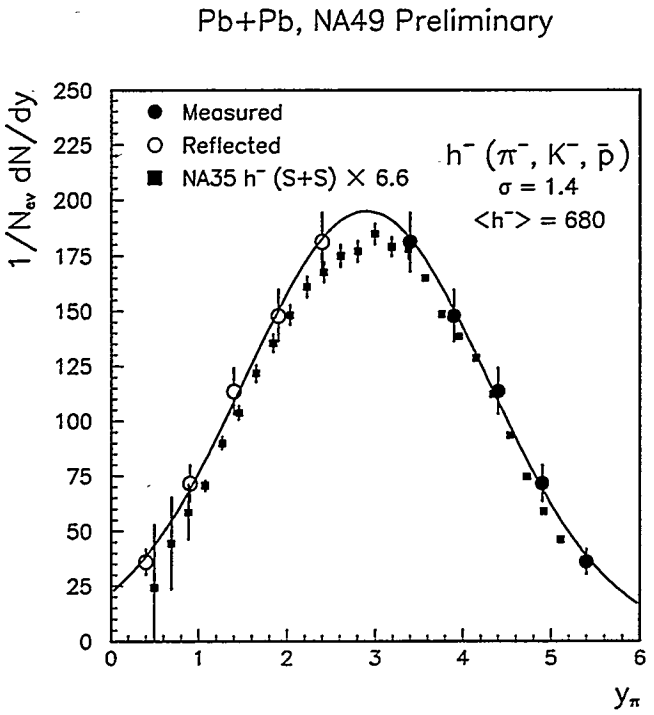

Figure 3: Rapidity density of negative hadrons for central collisions. Filled circles are NA49 measurement of Pb+Pb; open circles are same data reflected about mid-rapidity; filled squares are S+S from NA35 scaled by 6.6, the relative number of participants. Curve is Gaussian fit to Pb+Pb data; integral gives total negative hadron multiplicity of 680. Error bars include an estimate of systematic errors.

ring from the E_T deposited in its cells. The tensor is diagonalized to find the azimuthal orientation of major axis of deformation. The azimuthal orientation of the axis for either ring is uniformly distributed. The distribution of the relative azimuthal orientation of the forward and backward rings in an event, $\Delta\phi_{fb}$, is parametrized by the function

$$f(\Delta\phi_{fb}) = c * (1 + a_2 * cos(2\Delta\phi_{fb})). \quad (1)$$

Fig. 4 shows the strength of the correlation, given by coefficient a_2, as a function of centrality measured by the NA49 Veto (zero degree) calorimeter. The a_2 shows a strong impact parameter dependence and peaks at an impact parameter of about 8 fm. Also shown are predictions of the Venus [17] and RQMD [18] models filtered with the calorimeter response, as well as the Venus model with transverse momentum components for each particle modified to fit the observed a_2 behaviour while conserving energy and momentum. The fit can be summarized by a deformation parameter $R_p = 1.2$ at b=8 fm., where

$$R_p = \frac{< p_y^2 > - < p_y >^2}{< p_x^2 > - < p_x >^2}. \quad (2)$$

At these high energies it seems unlikely that the observed correlation is due to shad-

Particle	Pb–Pb		S–S	
	NA49 (preliminary)	NA44 (preliminary)	NA35	NA44 (preliminary)
π^+	188±6	156±6		148±4
π^-	192±3	154±8	197±14 [7]	148±4
K^+	244±12	234±6	227±15 [11]	180±8
K^-	213±6	235±7	190±22 [14]	180±7
K^0_s	223±13		210±16 [11]	
p	301±18	289±7	180±14 [7]	208±8
$\overline{p}$	291±24	278±9	184±14 [7]	190±7
Λ	293±10		204±17 [11]	
$\overline{\Lambda}$	288±10		180±24 [11]	

Table 1: Inverse slope parameters in GeV at mid–rapidity for a variety of species in central S+S and Pb+Pb collisions, from NA44 and NA49.

owing by the spectator matter, thought to generate the squeeze–out phenomenon at the Bevelac [19]. Rather, the explanation may lie in the persistence of memory by the participants of the initial conditions of the reaction [20]. Observation of a significant dipole moment of the E_T distribution at forward rapidity and its correlation with the quadrupole moment observed at mid–rapidity will clarify this.

4. Coulomb Effects

Fig. 5 shows measurements from NA44 of the ratio of yields of π^- and π^+ at mid–rapidity for central collisions of a variety of systems, as a function of $m_T - m_\pi$. Since Pb+Pb is the most asymmetric system in isospin, it is expected to have the largest excess of π^- over π^+. However, the figure shows the striking effect that for Pb+Pb this enhancement occurs preferentially at low $m_T - m_\pi$, but not for the lighter systems. This effect can be reproduced by a modified RQMD plus Coulomb calculation, with longitudinal co–moving charge $Z_{eff} = 40$ [13]. The bulk of the effect in the calculation is attributable to the presence of excess charge rather than hyperon decays.

NA49 has measured the two–particle correlation function C^{+-} between unlike–sign hadrons as a function of Q_{inv}. Under the assumption that this correlation is dominated by Coulomb effects, it can be used to study the recipes used to Coulomb–correct like–sign correlation functions. The net charge of the fireball may have considerable effect in very heavy systems and should be accounted for. The standard two–particle Gamov function clearly does not describe C^{+-}, whereas the phenomenological function with an exponential cutoff,

$$F(Q_{inv}) = 1 + (G^{+-}(Q_{inv}) - 1)e^{-Q_{inv}/Q_f}, \tag{3}$$

fits the data well. $G^{+-}(Q_{inv})$ is the standard Gamov function, and Q_f=75 MeV is a parameter that is fit to the data. Alternatively, a correction factor for the finite size of the

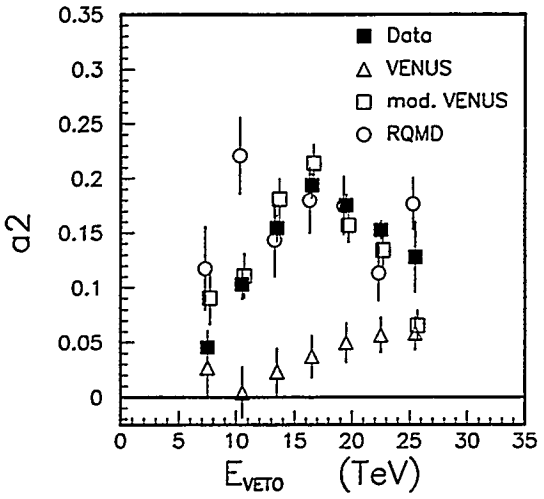

Figure 4: Coefficient a_2 from eq. 1 as a function of centrality (filled squares). Central collisions correspond to low E_{veto}, peripheral collisions to high E_{veto}. Also shown: predictions of the Venus (open triangles) and RQMD (open circles) models, as well as modified Venus (open squares; see text).

system can be obtained by integrating the Coulomb wavefunction of the observed pair over the finite volume of the source [21]. The data are well described by a source size of 5 fm. Both the net charge and finite size effects must come into play at some level, but await a unified treatment.

5. Conclusions

Central Pb+Pb collisions at 158 GeV/nucleon exhibit greater stopping than lighter systems at the same energy but less stopping than heavy systems at lower energies. Some of the extra energy available at mid–rapidity is taken up by greater radial flow. Medium impact parameter collisions reveal an asymmetric azimuthal distribution of transverse energy at mid–rapidity, indicating the preservation of the memory by the participants of the initial geometry of the collision. Significant Coulomb effects at low m_T in single particle distributions and in correlation measurements indicate the necessity to fully account for the effect of residual charge and finite size of the fireball.

6. Acknowledgements

I thank Nu Xu for making preliminary NA44 data available.

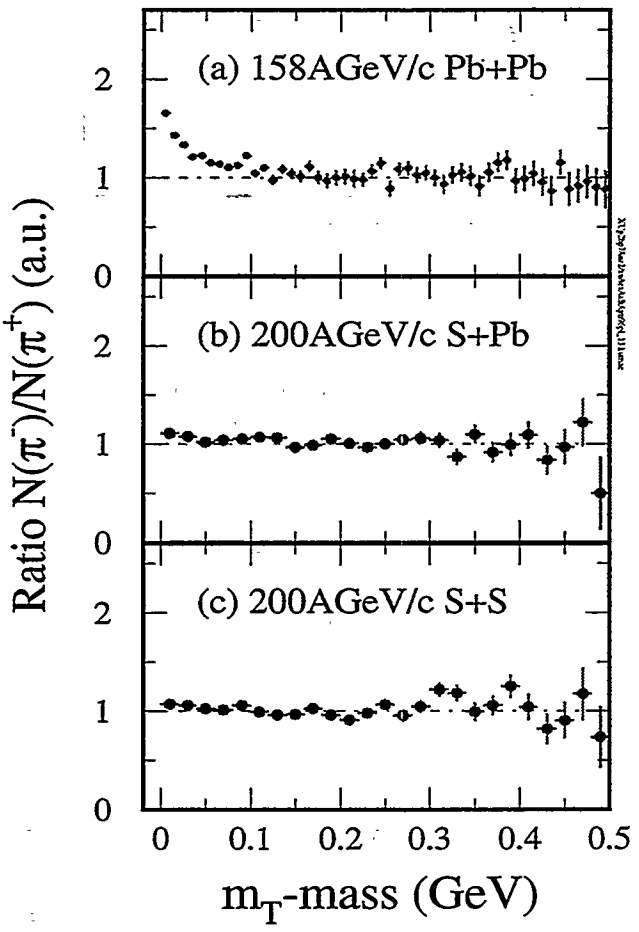

NA44, Phys. Lett. B, in press.

Figure 5: Ratio of the yields of π^- and π^+ at mid-rapidity for central collisions as a function of $m_T - m_\pi$, measured by NA44 for several systems. Ratio is normalized to 1 at high $m_T - m_\pi$.

7. References

1. P. Bordalo *et al.* (NA50 Collaboration), Proceedings of Rencontres de Moriond, ed. J. Tranh Tan Van (1996); M. Gonin *et al.* (NA50 Collaboration), Proceedings of Quark Matter 96, Heidelberg, Germany, May 20-24, 1996.
2. J.-P. Blaizot and J.-Y. Ollitraut, Phys. Rev. Lett. **77** 1703 (1996); S. Gavin and R. Vogt, LBL-37980.
3. Cern Courier **36** 1 (July/August 1996).
4. G. Taubes, Science **273** 1492 (13 September 1996).
5. See instead the proceedings of the recent Quark Matter conferences.
6. W. Busza and A. S. Goldhaber, Phys. Lett. **139B** 235 (1984).
7. J. Baechler *et al.* (NA35 Collaboration), Phys. Rev. Lett. **72** 1419 (1994).
8. T. Alber *et al.* (NA49 Collaboration), Phys. Rev. Lett. **75** 3814 (1995).
9. T. Wienold *et al.* (EOS Collaboration), to be published.
10. F. Videbæck *et al.* (E866 Collaboration), Nucl. Phys. **A590** 249c (1995).
11. T. Alber *et al.* (NA35 Collaboration), Z. Physik **C64** 195 (1994).
12. A. Bialas *et al.*, Nucl. Phys. **B111** 461 (1976); A. Bialas and B. Muryn, Acta Phys. Pol. **B18** 591 (1987).
13. Nu Xu *et al.* (NA44 Collaboration), Proceedings of Quark Matter 96, Heidelberg, Germany, May 20-24, 1996.
14. S. Margetis *et al.* (NA35 Collaboration), Proceedings of Strangeness 96, Budapest, Hungary, May 15-17, 1996.
15. J. Barrette *et al.* (E877 Collaboration), Phys. Rev. Lett. **73** 2532 (1994); see also W.-C. Chen *et al.*, these proceedings.
16. T. Wienold *et al.* (NA49 Collaboration), Proceedings of the 12th Winter Workshop on Nuclear Dynamics, Snowbird, Utah, Feb. 3-10, 1996.
17. K. Werner, Phys. Rep. **232** 87 (1995).
18. H. Sorge, Phys. Rev. **C52** 3291 (1995).
19. H. H. Gutbrod *et al.*, Phys. Lett. **B216** 267 (1989).
20. P. Filip, LANL Preprint hep-ex/9605001.
21. S. Pratt, Phys. Rev. **D33** 72 (1986).